

## Formation of Metastable Triplet Acetylene from the $\tilde{A}(^1A_u)$ State Near the Dissociation Threshold

Yang Shi<sup>†</sup> and Toshinori Suzuki\*

Institute for Molecular Science, Myodaiji, Okazaki 444-8585, Japan

Received: May 18, 1998; In Final Form: July 9, 1998

The triplet metastable states of acetylene produced by intersystem crossing from the  $\tilde{A}(^1A_u)$  state have been detected by a sensitized phosphorescence (SP) method. The phosphorescence was observed from  $C_2H_2$  in the energy region below the barrier to dissociation in the  $\tilde{a}$  state suggested by Hashimoto and Suzuki [*J. Chem. Phys.* **1996**, *104*, 6070]. The lifetimes of the triplet states coupled with the  $V^3K^1$  and  $V^4K^1$  levels in the  $\tilde{A}(^1A_u)$  state were estimated to be 80 and 100  $\mu s$ . The rotational structures of the laser-induced fluorescence and SP spectra were similar, except that the enhancement of many weak absorption lines makes the latter more congested. The feature of the SP spectrum exemplifies the complicated singlet–triplet mixing at the  $V^3K^1$  level. The SP signal was observed with different phosphors, where benzil was found to be the most sensitive. The SP spectrum of  $C_2D_2$  was observed only by using benzil. In addition to SP, the collision of metastable triplet acetylene with a phosphor surface yielded fluorescence. This is most likely to be fluorescence from the  $\tilde{A}(^1A_u)$  state of acetylene. The lifetime of the triplet states and the threshold energy to dissociation in  $C_2H_2$  and  $C_2D_2$  suggest that tunneling occurs on the  $\tilde{a}$  state and that the energy barrier to dissociation is higher than the previous estimation.

### Introduction

Acetylene is one of the most important hydrocarbon molecules and its photophysics and photochemistry receive extensive attention. In particular, the interaction between the singlet and triplet states has been studied by a number of researchers.

Field and co-workers reported first the long-lived emission ( $\tau \approx 2 \mu s$ ) and the quantum beat from the  $V^3K^1$  level in the  $\tilde{A}(^1A_u)$  state,<sup>1</sup> where V denotes an in-plane trans-bending mode ( $\nu_4$  in the  $\tilde{X}$  and  $\nu_3$  in the  $\tilde{A}$  states) and K is the projection of angular momentum on the *a* axis. Wolff and Zacharias observed biexponential fluorescence decay with lifetimes of several hundred nanoseconds and several microseconds for a number of rovibronic levels in the  $\tilde{A}$  state.<sup>2</sup> Ochi and Tsuchiya studied extensively the Zeeman beat and biexponential decay in the magnetic field.<sup>3</sup> From the analysis of the Zeeman beat, they proposed the direct coupling between  $\tilde{A}$  and  $\tilde{c}$  the indirect coupling between  $\tilde{A}$  and  $\tilde{b}$  mediated by the  $\tilde{c}-\tilde{b}$  interaction.<sup>3</sup> This suggestion was in accord with ab initio calculations by Lischka and Karpfen that showed the curve crossing between the  $\tilde{A}(^1A_u)$  and  $\tilde{c}(^3B_u)$  states in the planar geometry.<sup>4</sup> Dupré and co-workers measured the Zeeman anticrossing (ZAC) spectra and observed enormous density of states, 100 times larger than the maximum density expected for the  $\tilde{a} \sim \tilde{c}$  triplet states, interacting with the  $V^3K^1$  level.<sup>5–7</sup> Abe and Hayashi observed the quenching of the  $V^nK^1$  ( $n = 1–4$ ) levels in the magnetic field.<sup>8</sup> Drabbels et al. performed high-resolution laser-induced fluorescence (LIF) spectroscopy and suggested that the  $\tilde{a}(^3B_u)$  state is coupled with the  $\tilde{A}(^1A_u)$  state.<sup>9</sup> They ascribed the high state density observed by ZAC to the ground-state levels interacting with the  $\tilde{A}$  state.<sup>9</sup>

The essential role of the interaction between the  $\tilde{A}(^1A_u)$  and  $\tilde{a}(^3B_u)$  states in the predissociation process of acetylene has been

revealed by Hashimoto and Suzuki<sup>10</sup> and Ashfold and co-workers.<sup>11,12</sup> These works have shown that predissociation occurs from the  $\tilde{A}(^1A_u)$  state to  $C_2H(X^2\Sigma^+) + H(^2S)$  even though these are not adiabatically correlated, indicating that dissociation is mediated by electronic relaxation. Furthermore, systematic investigations of the translational energy release revealed that there is an exit energy barrier to dissociation.<sup>10,11</sup> Such a barrier is not expected for dissociation from the ground state but is possible for dissociation from the  $\tilde{a}$  state due to the avoided crossing with the  $^3(\sigma, \sigma^*)$  state.<sup>10</sup> Thus, it has been suggested that the predissociation near the threshold is induced by intersystem crossing. Recently, Morokuma and co-workers have shown the possible predissociation pathway via the triplet manifold by ab initio calculations, in agreement with the experimental observation.<sup>13,14</sup>

The present paper describes direct observation of metastable triplet acetylene produced by intersystem crossing (ISC) from the  $\tilde{A}(^1A_u)$  state by sensitized phosphorescence (SP) spectroscopy, thereby confirming the proposed dissociation mechanism via the triplet manifold. Preliminary results have been reported previously.<sup>15</sup> More recently, Field, Wodtke and co-workers have also detected the metastable triplet acetylene by the Auger method.<sup>16</sup> The results obtained by the two methods are compared.

### Experimental Section

The basic design of our apparatus, shown in Figure 1, is similar to those described by Abe et al.<sup>17</sup> and Kume et al.<sup>18</sup> An Al coldfinger (surface area 18 cm<sup>2</sup>) cooled to liquid-nitrogen temperature was placed 50 mm downstream from the laser–jet interaction region at an angle of 45° to the centerline of the jet. A supersonic jet was formed by expanding  $C_2H_2$  seeded in He or Ar using a piezoelectric pulsed valve.<sup>19</sup> The typical stagnation pressure was 1 atm relative to the vacuum. The vacuum

<sup>†</sup> Present address: Department of Chemistry, University of Nevada, Reno.

\* Corresponding author. electronic mail: suzuki@ims.ac.jp.

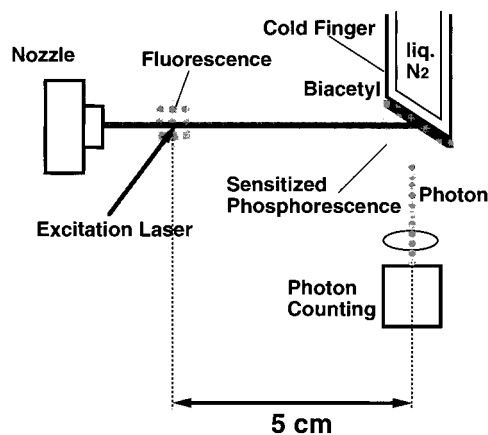


**Figure 1.** Schematic diagram of sensitized phosphorescence spectroscopy.

chamber was evacuated by a 700 L/s oil diffusion pump (Edwards, Diffstak). The pressure in the chamber was  $1 \times 10^{-5}$  Torr when operating the pulsed valve at 10 Hz. The laser beam was the second harmonic of the output of a Nd:YAG pumped dye laser (Spectra Physics GCR 170 and Lumonics HD500, Stilbene 420, Coumarin 440, and Coumarin 460) generated in a  $\beta$ -BaB<sub>2</sub>O<sub>4</sub> (BBO) crystal. The resolution of the laser was estimated to be about  $0.2 \text{ cm}^{-1}$  in the second harmonic. The laser beam ( $\sim 40 \mu\text{J}/\text{pulse}$ ) was introduced into the chamber without any focusing lens and crossed with the jet 10 mm downstream from the nozzle. A PIN photodiode was used as a laser power monitor.

LIF was observed with standard collection optics, a color filter (Corning 7-54), and a photomultiplier tube (PMT) (Hamamatsu, R928). The output signal from the PMT was preamplified, averaged for 5–10 laser shots by a boxcar integrator (Stanford Research Systems, SR250), and recorded in a computer.

When metastable triplet species produced by ISC from the optically excited state strikes the phosphor surface, energy transfer from the metastable triplet molecule to the phosphor brings about phosphorescence; thus ISC is detected.<sup>20–22</sup> Various molecules, such as biacetyl and benzil, were employed as phosphors. The vapor of a liquid phosphor was introduced from the second pulsed valve (General Valve, 9, 0.8 mm orifice diameter) located near the surface at the repetition rate of less than 1 Hz, to refresh the surface during the experiment. Solid phosphors distilled in alcohol were deposited on the Al surface and installed in the vacuum chamber. As the cold solid phosphor was in the vacuum for 12 h, a uniform phosphor layer grew, presumably due to diffusion on the surface and a sublimation–condensation cycle. The emission from the phosphor surface was detected by collection optics and a thermoelectrically cooled photon-counting PMT (Hamamatsu R928, C-2761, 2762). A series of color filters (Hoya UV28–IR70) were used in front of the PMT in order to estimate the wavelength range of emission and later to remove scattered light. The output of the PMT was fed into a gated photon counter (SRS SR400). The background noise was discriminated to be less than 10 counts/s. The gate width was set individually for different emission lifetimes of the phosphors. The time gate of 0.3–6 ms after the laser pulse was adopted for biacetyl. The time profiles of sensitized phosphorescence were recorded by a multichannel scaler (SRS SR430).

C<sub>2</sub>H<sub>2</sub> (Kansai 99.99%) was used without further purification. C<sub>2</sub>D<sub>2</sub> was synthesized from CaC<sub>2</sub> (Wako, 99.9%) and D<sub>2</sub>O (Wako, AR) and used after passing through a chloroform/liquid

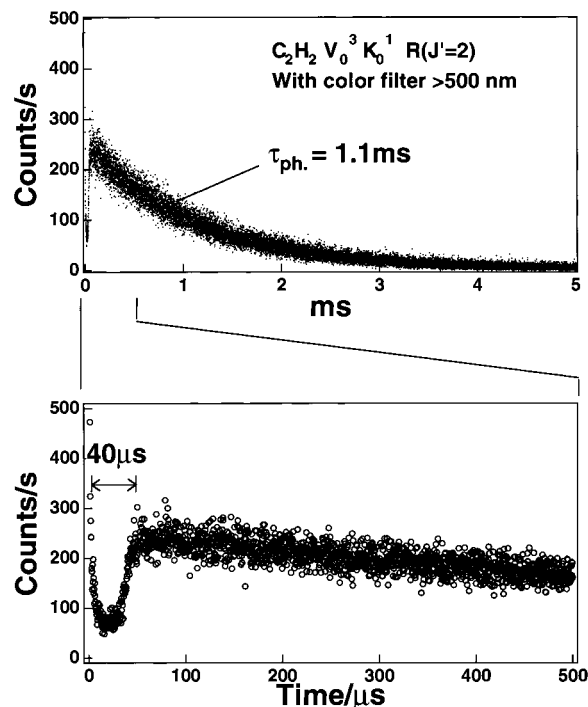


**Figure 2.** Emission time profile of biacetyl surface at liquid nitrogen temperature. The emission was observed through a color filter that passes the visible light  $\lambda > 500 \text{ nm}$ .

N<sub>2</sub> trap ( $-63.5 \text{ }^\circ\text{C}$ ). All phosphors (purity,  $>98\%$ ) were used without further purification.

## Results

**A. Sensitized Phosphorescence from Biacetyl.** A typical time profile of sensitized phosphorescence is shown in Figure 2. The emission was observed through the color filter that permits the transmission of the visible light,  $\lambda > 500 \text{ nm}$ .<sup>22</sup> The signal rises about  $40 \mu\text{s}$  after the laser pulse and decays slowly with a lifetime of 1.1 ms. It is known that the phosphorescence lifetime of biacetyl on the surface is different from those in the solid (2.6 ms) and vapor (1.8 ms) phases.<sup>23,24</sup> The variation of the lifetime as a function of the thickness of the biacetyl layer has been investigated by Alivisatos et al. for biacetyl/NH<sub>3</sub>/Ag-(111).<sup>23</sup> The rise at  $40 \mu\text{s}$  is given by the flight time of acetylene from the laser–molecular beam interaction region to the surface, and it has shifted to  $85 \mu\text{s}$  for acetylene seeded in Ar. The strong emission just after the laser pulse is the scattered light of fluorescence.

Figure 3 shows the LIF and SP spectra measured for the  $V_0^1 K_0^1$  ( $n = 2–4$ ) bands of the  $\tilde{A}^1A_u - \tilde{X}^1\Sigma_g^+$  transition of acetylene.<sup>25–36</sup> The relative intensities of the LIF and SP spectra in the figure are arbitrary. The distinct and confined rotational structures indicate that the observed LIF and SP spectra are due to jet-cooled C<sub>2</sub>H<sub>2</sub>. The results clearly show that ISC occurs from the  $\tilde{A}$  state. The SP signal was not observed for the  $V_0^5 K_0^1$  band, suggesting that the triplet states produced from this level are short-lived. This is in accord with the speculation by Hashimoto and Suzuki that the triplet level coupled to the  $V^5K^1$  level is located above the dissociation barrier to C<sub>2</sub>H( $2\Sigma^+$ ) + H.<sup>10</sup> The reaction time from the  $V^5K^1$  level has been estimated to be less than 70 ns by the pump–probe experiment.<sup>37</sup>

The rotational structures of the LIF and SP spectra are different, reflecting the fluorescence quantum yield that decreases with the rotational quantum number  $J$ .<sup>10,38,39</sup> Close inspection of the  $V_0^3 K_0^1$  band shown in Figure 4 reveals that SP

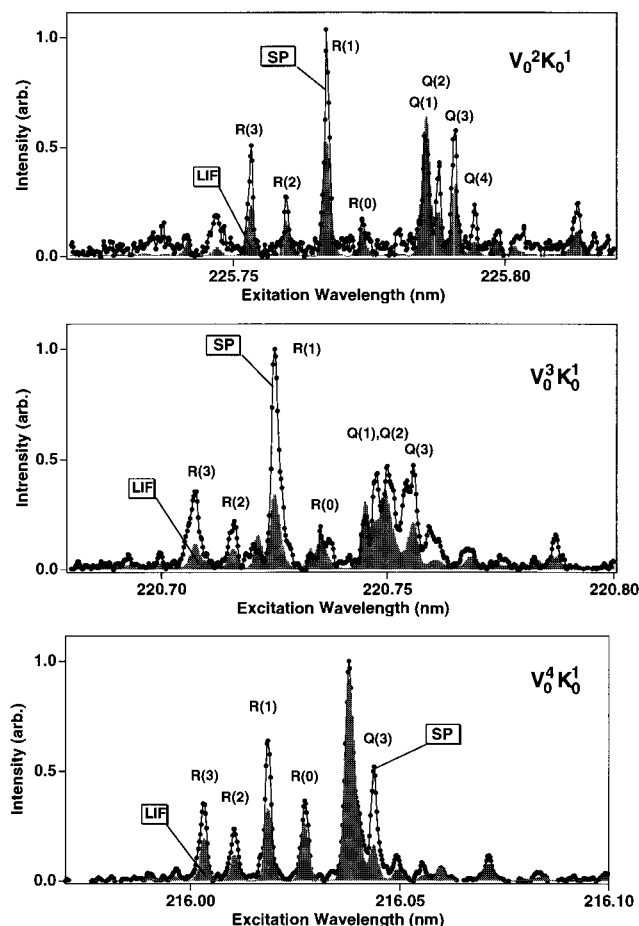


Figure 3. LIF and SP spectra of the bands.

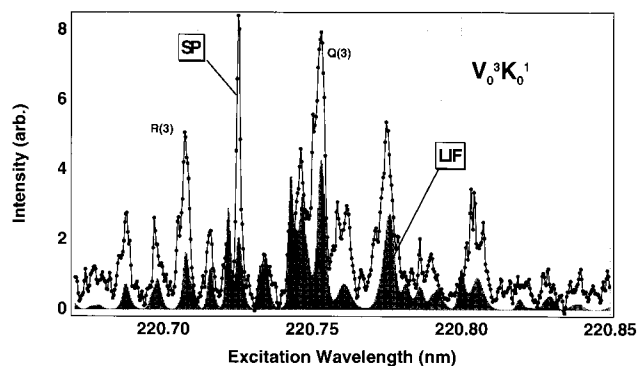


Figure 4. Expanded view of the LIF and SP spectra of the band measured for pure  $C_2H_2$ .

spectroscopy is more sensitive to the weak absorption lines than is LIF. Marked difference between the LIF and SP spectra exemplifies the strong variation of the triplet characters among the rotational states at the  $V^3K^1$  level, in agreement with the Zeeman beat, ZAC, and high-resolution LIF spectroscopies.<sup>3–9</sup>

The  $V^3K^1$  level has the Fermi interaction with the  $\nu_2 + 2\nu_4$  level.<sup>1b</sup> Drabbels et al. have shown the upper state attributed to the  $\nu_2 + 2\nu_4$  level exhibits a much smaller interaction with the triplet states.<sup>9</sup> In accordance with this earlier report, the simultaneous measurement of LIF and SP revealed that the  $\nu_2 + 2\nu_4$  levels exhibit a larger LIF/SP intensity ratio than do the  $V^3$  levels. The smaller singlet–triplet interaction at the  $\nu_2 + 2\nu_4$  level has been attributed to the unfavorable Franck–Condon overlap with the cis triplet ( $^3B_2$ ) state.<sup>5,9</sup>

**B. Lifetime and Yield of Triplet Acetylene.** To estimate the lifetimes of the triplet states produced by ISC, the signal intensity was measured for different flight times by changing the carrier gas, where the angular divergence of the molecular beam was assumed to be the same. When the SP intensities of acetylene seeded in He and Ar were compared, the lifetimes of the triplet states produced by ISC from the  $V^3K^1$  ( $J' = 2$ ) and  $V^4K^1$  ( $J' = 2$ ) levels were estimated to be 100 and 80  $\mu s$ , respectively. The experimental error is estimated to be about 50  $\mu s$ . The lifetimes of the triplet states were the same for different rotational levels within the experimental error.

Hunziker and co-workers have suggested the lifetime of 30  $\mu s$  for the  $^3B_2$  state of *cis*-acetylene.<sup>40</sup> On the other hand, Lisy and Klemperer have suggested  $\tau > 1$  ms for the *trans* triplet.<sup>41</sup> From these results, it has been speculated that the *cis* triplet has a much shorter lifetime than the *trans* triplet. According to ab initio calculations,<sup>13,14,42–44</sup> the  $\bar{a}$  state lies higher than the *cis*–*trans* isomerization barrier in the  $\bar{a}$  state so that triplet acetylene produced by ISC can interconvert freely between the *cis* and *trans* structures. Therefore, the fact that the triplet acetylene produced by ISC has a lifetime as long as 100  $\mu s$  suggests that the lifetime of *cis*-acetylene at the zero vibrational level in the state is longer than 30  $\mu s$ . On the contrary, if this lifetime is correct, then our assignment of the triplet detected in the state should be reexamined.

The relative ISC yield,  $\Phi_{ISC}$ , is estimated from the observed SP intensity and the lifetimes of the triplet states as follows:

$$\Phi_{ISC} \approx I_{phos} \exp\left(\frac{t_{flight}}{\tau_T}\right) \Phi_{fluo} / I_{fluo}$$

Here,  $I_{phos}$  is the intensity of sensitized phosphorescence and  $\tau_T$  is the lifetime of the triplet state produced by ISC. Without the lifetime correction, the SP intensities at a flight time of 85  $\mu s$  were 1, 0.6, and 0.2 for the  $V^2K^1$  ( $J' = 2$ ),  $V^3K^1$  ( $J' = 2$ ), and  $V^4K^1$  ( $J' = 2$ ) levels, respectively. The R(1) lines were used in all the measurements. Taking into account the lifetimes of the  $V^3K^1$  ( $J' = 2$ ), and  $V^4K^1$  ( $J' = 2$ ) levels of 100 and 80  $\mu s$ , respectively, the ratio of  $\Phi_{ISC}$  for these levels is 1:0.41. Thus, the ISC yield is estimated to be on the same order for the  $V^3K^1$  and  $V^4K^1$  levels. The relative ISC yields at the  $V^2K^1$  and  $V^4K^1$  levels, shown in Figure 5, do not depend on the rotational states. (The  $V^3K^1$  level was omitted because of the highly complicated and congested feature of the  $V_0^3K_0^1$  band.)

**C. Other Phosphors.** We observed the SP spectrum with the phosphors listed in Table 1. Acetone, benzene, and naphthalene did not provide the SP signal, which is presumably due to the relatively small phosphorescence quantum yields of these molecules, 0.03, 0.18, and 0.07 in EPA glass (77 K) for acetone, benzene, and naphthalene, respectively.<sup>45</sup> The observed phosphorescence lifetime was always longer at liquid  $N_2$  temperature than at room temperature due to the temperature dependence of the nonradiative processes of  $T_1 \rightarrow S_0$  and  $T_1 \rightarrow S_1$ ,  $k = k_r + k_{nr} \exp(-E_a/kT)$ .

We found that benzil provides a 1 order of magnitude stronger SP signal than does biacetyl. The SP spectrum of  $C_2D_2$  could be observed only by using benzil as a phosphor, as shown in Figure 6. However, the low signal level did not allow us to determine the lifetimes of the triplet states of  $C_2D_2$ . The SP signal was observed up to the  $1_{0_2}^1V_0^2K_0^1$  band. Fujii and co-workers have reported that the fluorescence quantum yield of  $C_2D_2$  falls off between  $1_{0_2}^1V_0^2K_0^1$  (47 427  $cm^{-1}$ ) and  $1_{0_1}^1V_0^1K_0^1$  (47 505  $cm^{-1}$ ) bands. The SP intensity diminished in the same region.

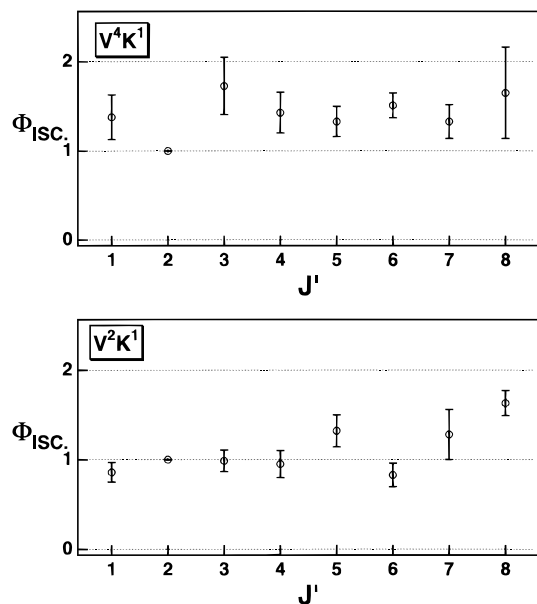


Figure 5. Rotational state dependence of the ISC yield at the  $V^2K^1$  and  $V^4K^1$  levels. R branch was used.

TABLE 1: List of Phosphors Used

sample	$E_T/eV^a$	sensitized phosphorescence <sup>b</sup>	obsd lifetime/ms
benzene	3.6	—	
acetone	3.4	—	
acetophenone	3.2	+	1.6 (77 K)
benzophenone	3.0	+	2.0 (77 K)
thioxanthene-9-one	2.8	+	0.15 (300 K), 0.3 (77 K)
anthraquinone	2.7	+	0.25 (300 K), 2.2 (77 K)
naphthalene	2.6	—	
2-acetonaphthone	2.6	+	2.3 (77 K)
biacetyl	2.4	+	1.1 (77 K)
benzil	2.3	+	0.12 (300 K) 2.0 (77 K)
pyrene	2.1	—	

<sup>a</sup> Energy of the lowest triplet state. <sup>b</sup> + and — mean whether or not the SP signal was observed.

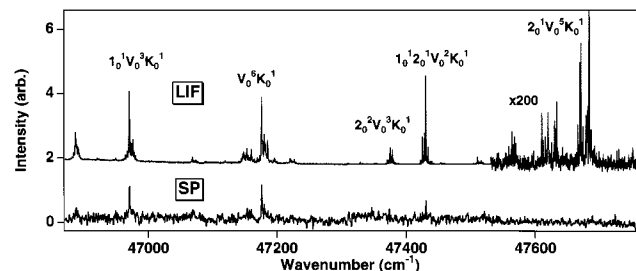


Figure 6. LIF and SP spectra of  $C_2D_2$  measured simultaneously. Benzil at the liquid nitrogen temperature was used as a sensitizer.

**D. Collision-Induced Emission.** When sensitized phosphorescence was observed without a color filter, a sharp peak appeared in the time profile, as shown in Figure 7a. The peak position,  $37 \mu s$ , corresponded to the arrival time of metastable acetylene at the surface. Close inspection reveals that the peak shape is symmetric and triangular. This shape is only possible for an emission lifetime less than  $2.5 \mu s$ . Such a short-lived emission must be fluorescence. By use of different color filters, the emission wavelength was estimated to be shorter than 500 nm. (That is why the peak was not seen in Figure 2.)

As seen in Figure 7b–d, the fluorescence was observed for all the phosphors used and even without any phosphor on the surface. The fluorescence quantum yields of the phosphors are too low to be responsible for the observed fluorescence.

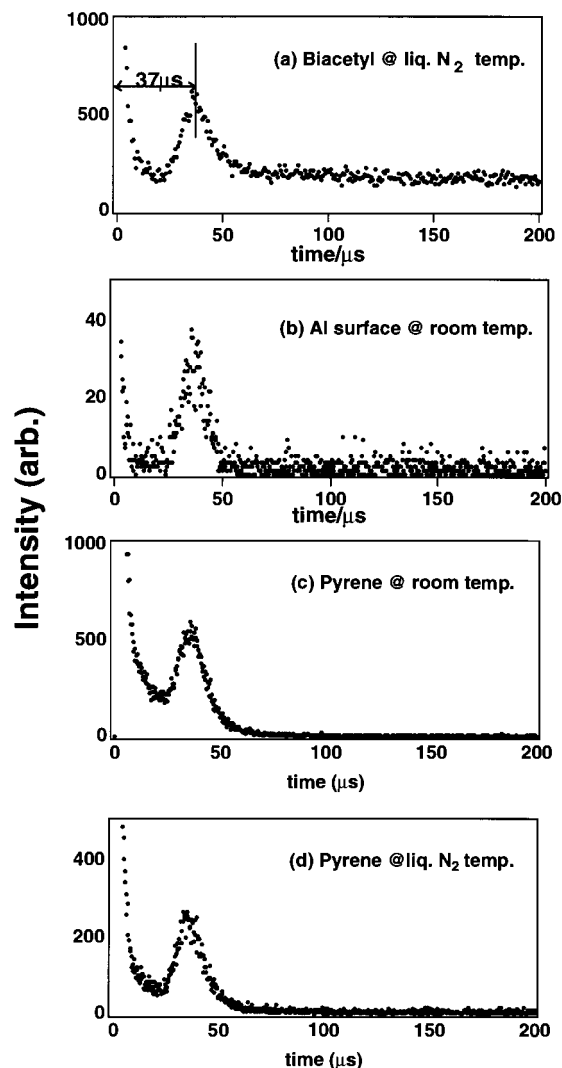


Figure 7. Emission time profiles of (a) biacetyl surface at liquid  $N_2$  temperature, (b) Al surface at room temperature, (c) pyrene surface at room temperature, and (d) pyrene surface at liquid  $N_2$  temperature. Emission was observed without any color filter.

Therefore, the fluorescence is most likely from acetylene due to the collision-induced  $T \rightarrow S$  ISC. The fluorescence lifetime of acetylene is less than  $2 \mu s$  and the emission wavelength is in the 250–450 nm<sup>46</sup> range that is in accord with the observation. Nevertheless, an impurity on the surface cannot be completely ruled out as the source of the fluorescence. Dispersed emission spectroscopy will elucidate it.

Figure 8 shows the  $V_0^4K_0^1$  band observed by LIF and collision-induced fluorescence (CIF). The spectral feature of CIF is in agreement with the SP spectrum shown in Figure 3, indicating that both methods monitor the same metastable species.

The CIF was also examined for  $\tilde{a} \leftarrow \tilde{X}$  direct absorption of glyoxal. By excitation of glyoxal to the zero vibrational level in the  $\tilde{a}$  state, CIF was observed using the Al surface at room temperature. The energy difference between the  $\tilde{A}$  and  $\tilde{a}$  states in glyoxal is  $2774.8 \text{ cm}^{-1}$ , while the collision energy of glyoxal with the surface was more than  $6000 \text{ cm}^{-1}$ , allowing the collision-induced ISC energetically.

## Discussion

**A. Character of the Metastable State.** The singlet state with the emission lifetime of  $2 \mu s$  decays by  $10^{-9}$  and  $10^{-18}$  in



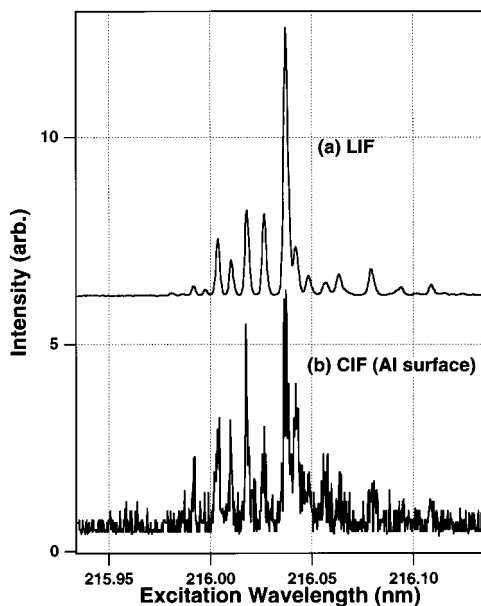


**Figure 8.** LIF and CIF spectra of the band. A bare Al surface at room temperature was used.

the flight times of 40 and 80  $\mu\text{s}$ , respectively. Therefore, sensitized phosphorescence must arise from a long-lived triplet state. The estimated lifetime of 100  $\mu\text{s}$  is in accord with this expectation. Field, Wodtke, and co-workers have detected metastable species by the Auger method using gold ( $\phi = 5.1$  eV).<sup>16</sup> The lifetimes estimated by the SP and Auger methods are in excellent agreement, suggesting that the two methods monitor the same species. They claimed that the Auger method using gold is only sensitive to the  $\tilde{c}$  state (and the  $\tilde{A}$  state), since it is located above 5.1 eV. On the other hand, the SP method is sensitive to all the triplet states of acetylene, since the triplet state of biacetyl is lower than any of the triplet states of acetylene.

The agreement of the lifetime measured by the two methods may suggest that both observe the  $\tilde{c}$  state. However, this is not the unique explanation. For instance, when a metastable species strikes the surface, collision-induced processes may scramble the electronic state. If this occurs, the electronic state of the metastable state cannot be assigned easily. CIF given by the collision of triplet molecules with the surface may point to this possibility. The  $\tilde{c}$  ( ${}^3B_u$ ) and  $\tilde{b}$  ( ${}^3A_u$ ) states are the Renner–Teller pairs of the  ${}^3\Delta_u$  state, and nonadiabatic transition occurs between them in the linear geometry. Furthermore, these states are

coupled to the  $\tilde{a}$  state as evidenced by the large triplet-level density interacting with the  $\tilde{A}$  state observed by the Zeeman beat and LIF spectroscopies. Thus, acetylene is most likely in the  $\tilde{a}$  state in collision with the surface but is partially converted to the  $\tilde{A}$  and/or  $\tilde{c}$  states. Therefore, it is speculated that both the SP and Auger methods are sensitive to all the triplet states.

There is a difference between the spectra obtained by the SP and the Auger methods. The spectrum observed by the Auger method shows a broad background, while the SP spectrum does not, even though the SP spectrum is more congested than the LIF. The origin of this discrepancy is not understood yet.

**B. Tunneling Through the Barrier.** The lifetime of the triplet metastable state produced from the  $V^4K^1$  level was estimated to be 80  $\mu\text{s}$ . The result implies that the tunneling through the barrier in the state is negligible at this energy ( $E_{\text{excess}} = 220$   $\text{cm}^{-1}$ ). We estimated the tunneling probability  $P(E)$  by assuming an asymmetric Eckart barrier for which analytical forms of  $P(E)$  are available.<sup>47,48</sup> For the reverse reaction barrier of 560  $\text{cm}^{-1}$  (ref 10) and the imaginary frequency of 1114  $\text{cm}^{-1}$ ,<sup>14</sup> the  $P(E)$  at 340  $\text{cm}^{-1}$  below the barrier (corresponding to the  $V^4K^1$  level) is calculated to be as large as 0.11. For the barrier height of 1000  $\text{cm}^{-1}$ , the  $P(E)$  is 0.004. The results suggest that the potential barrier is higher and/or thicker than the Eckart barrier assumed.

Fujii and co-workers have reported that fluorescence sharply falls off between the  $V^4K^2$  and  $2^1V^3K^0$  levels in  $C_2H_2$  and between the  $1^2V^2K^1$  and  $1^2V^1K^1$  levels in  $C_2D_2$ .<sup>38,39</sup> Their results were reproduced in the present work. Furthermore, sensitized phosphorescence diminished in the same region. This suggests that broadening of the triplet states by dissociation causes the falloff of fluorescence. The falloff region is energetically higher in  $C_2D_2$  than in  $C_2H_2$  by about 960  $\text{cm}^{-1}$ , which is close to the difference of the zero-point vibrational energy in the ground state, 1156  $\text{cm}^{-1}$ . However, this is not understood by a classical model. From the zero-point energy difference between CCH and CCD, 527  $\text{cm}^{-1}$ ,<sup>49</sup> the zero-point energy difference between  $C_2H_2$  and  $C_2D_2$  at the transition state for dissociation is estimated to be about 600–700  $\text{cm}^{-1}$ . When this value is taken into account, the difference of the classical energy barrier to dissociation between  $C_2H_2$  and  $C_2D_2$  is expected to be about 550 (1200 – 650 = 550)  $\text{cm}^{-1}$ . The observed energy difference  $\sim 960$   $\text{cm}^{-1}$  is larger than this expectation, indicating that the threshold is effectively lower for  $C_2H_2$  because of the tunneling effect.

As shown in Figure 9, weak emission was observed from the  $1^2V^1K^1$  level ( $E_{\text{excess}} = 752$   $\text{cm}^{-1}$ ) in  $C_2D_2$ . Therefore, the

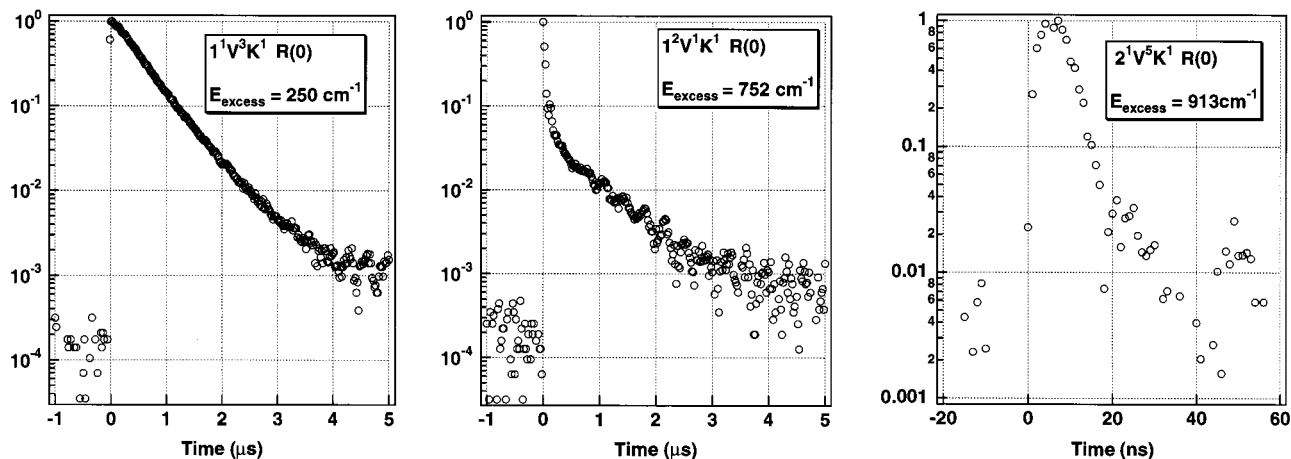


**Figure 9.** Fluorescence decay curves from (a)  $1^1V^3K^1$ , (b)  $1^2V^1K^1$ , and  $2^1V^5K^1$  levels of jet-cooled  $C_2D_2$ .

reverse reaction barrier is estimated to be slightly higher than  $752\text{ cm}^{-1}$  for  $\text{C}_2\text{D}_2$ .

**Acknowledgment.** We thank M. Herman (Université Libre de Bruxelles) for providing us with the compilation of the spectral assignment of the bands of  $\text{C}_2\text{H}_2$  and  $\text{C}_2\text{D}_2$ . We also thank K. Tsuji (Tokyo Institute of Technology) for sending us the unpublished results of the LIF measurements. This work was supported in part by a Grant-in-Aid from the Ministry of Education, Science, Sports and Culture (Contract Nos. 08559014 and 09440208) and the New Energy and Industrial Technology Development Organization.

## References and Notes

- (1) (a) Abramson, E.; Kittrell, C.; Kinsey, J. L.; Field, R. W. *J. Chem. Phys.* **1982**, *76*, 2293. (b) Sherer, G. J.; Chen, Y.; Redington, R. L.; Kinsey, J. L.; Field, R. W. *J. Chem. Phys.* **1986**, *85*, 6315.
- (2) Wolff, D.; Zacharias, H. *Chem. Phys. Lett.* **1990**, *174*, 563.
- (3) (a) Ochi, N.; Tsuchiya, S. *Chem. Phys. Lett.* **1987**, *140*, 20. (b) *Chem. Phys.* **1991**, *152*, 319.
- (4) Lischka, H.; Karpfen, A. *Chem. Phys.* **1986**, *102*, 77.
- (5) Dupré, P.; Jost, R.; Lombardi, M.; Green, P. G.; Abramson, E.; Field, R. W. *Chem. Phys.* **1991**, *152*, 293.
- (6) Dupré, P.; Green, P. G.; Field, R. W. *Chem. Phys.* **1995**, *196*, 211.
- (7) Dupré, P. *Chem. Phys.* **1995**, *196*, 239.
- (8) Abe, H.; Hayashi, H. *Chem. Phys. Lett.* **1993**, *206*, 337.
- (9) Drabbles, M.; Heinze, J.; Meerts, W. L. *J. Chem. Phys.* **1994**, *100*, 165.
- (10) Hashimoto, N.; Suzuki, T. *J. Chem. Phys.* **1996**, *104*, 6070.
- (11) Wilson, S. H. S.; Reed, C. L.; Mordaunt, D. H.; Ashfold, M. N. R.; Kawasaki, M. *Bull. Chem. Soc. Jpn.* **1996**, *69*, 71.
- (12) Mordaunt, D. H.; Ashfold, M. N. R.; Dixon, R. N.; Löffler, P.; Schnieder, L.; Welge, K. H. *J. Chem. Phys.* **1998**, *108*, 519.
- (13) Cui, Q.; Morokuma, K.; Stanton, J. F. *Chem. Phys. Lett.* **1996**, *263*, 46.
- (14) Cui, Q.; Morokuma, K. *Chem. Phys. Lett.* **1997**, *272*, 319.
- (15) Suzuki, T.; Shi, Y.; Kohguchi, H. *J. Chem. Phys.* **1997**, *106*, 5292.
- (16) Humphrey, S. J.; Morgan, C. G.; Wodtke, A. M.; Cunningham, K. L.; Drucker, S.; Field, R. W. *J. Chem. Phys.* **1997**, *107*, 49.
- (17) Abe, H.; Kamei, S.; Mikami, N.; Ito, M. *Chem. Phys. Lett.* **1984**, *109*, 217.
- (18) Kume, H.; Kondow, T.; Kuchitsu, K. *J. Chem. Phys.* **1986**, *84*, 4031.
- (19) Proch, D.; Trickl, T. *Rev. Sci. Instrum.* **1989**, *60*, 713.
- (20) Ahmed, M.; Callear, A. B. *Chem. Phys. Lett.* **1989**, *174*, 563.
- (21) Lind, S. C.; Jungers, J. C.; Schiflett, C. H. *J. Am. Chem. Soc.* **1935**, *57*, 1032.
- (22) Burton, C. S.; Hunziker, H. E. *J. Chem. Phys.* **1972**, *57*, 339.
- (23) Alivisatos, A. P.; Waldeck, D. H.; Harris, C. B. *J. Chem. Phys.* **1985**, *82*, 541.
- (24) (a) Dubois, J. T.; Wilkinson, F. *J. Chem. Phys.* **1963**, *39*, 899. (b) Moss, A. Z.; Yardley, J. T. *J. Chem. Phys.* **1974**, *61*, 2883. (c) Brand, J. C. D.; Mau, A. W. H. *J. Am. Chem. Soc.* **1974**, *96*, 4380. (d) Kaya, K.; Harshbarger, W. R.; Robin, M. B. *J. Chem. Phys.* **1974**, *60*, 4231.
- (25) Innes, K. K. *J. Chem. Phys.* **1954**, *22*, 863.
- (26) Ingold, C. K.; King, G. W. *J. Chem. Soc.* **1953**, 2702.
- (27) Watson, J. K. G.; Herman, M.; Van Craen, J. C.; Colin, R. *J. Mol. Spectrosc.* **1982**, *95*, 101.
- (28) Van Craen, J. C.; Herman, M.; Colin, R.; Watson, J. K. G. *J. Mol. Spectrosc.* **1985**, *111*, 185.
- (29) Van Craen, J. C.; Herman, M.; Colin, R.; Watson, J. K. G. *J. Mol. Spectrosc.* **1986**, *119*, 137.
- (30) Huet, T. R.; Herman, M. *J. Mol. Spectrosc.* **1988**, *132*, 261.
- (31) Van der Auwera, J.; Huet, T. R.; Herman, M.; Hamilton, C.; Kinsey, J. L.; Field, R. W. *J. Mol. Spectrosc.* **1989**, *137*, 381.
- (32) Huet, T. R.; Herman, M. *J. Mol. Spectrosc.* **1989**, *137*, 396.
- (33) Huet, T. R. Ph.D. Thesis, Université Libre de Bruxelles, 1990.
- (34) Utz, A. L.; Tobiason, J. D.; Carrasquillo, M. E.; Sanders, J. L.; Crim, F. F. *J. Chem. Phys.* **1993**, *98*, 2742.
- (35) Tobiason, J. D.; Utz, A. L.; Sibert, E. L.; Crim, F. F. *J. Chem. Phys.* **1993**, *99*, 5762.
- (36) Tobiason, J. D.; Utz, A. L.; Crim, F. F. *J. Chem. Phys.* **1993**, *99*, 928.
- (37) Hashimoto, N.; Yonekura, N.; Suzuki, T. *Chem. Phys. Lett.* **1997**, *264*, 545.
- (38) Fujii, M.; Haijima, A.; Ito, M. *Chem. Phys. Lett.* **1988**, *150*, 380.
- (39) Haijima, A.; Fujii, M.; Ito, M. *J. Chem. Phys.* **1990**, *92*, 959.
- (40) Wendt, H. R.; Hippler, H.; Hunziker, H. E. *J. Chem. Phys.* **1979**, *70*, 4044.
- (41) Lisy, J. M.; Klempner, W. *J. Chem. Phys.* **1980**, *72*, 3880.
- (42) Yamaguchi, Y.; Vacek, G.; Thomas, J. R.; DeLeeuw, B. J.; Shaefer, H. F. *J. Chem. Phys.* **1994**, *100*, 4969.
- (43) Stanton, J. F.; Gauss, J. *J. Chem. Phys.* **1994**, *101*, 3001.
- (44) Stanton, J. F.; Huang, C.-M.; Szalay, P. G. *J. Chem. Phys.* **1994**, *101*, 356.
- (45) Gilmore, E. H.; Gibson, G. E.; McClure, D. S. *J. Chem. Phys.* **1952**, *20*, 829.
- (46) Stephenson, J. C.; Blazy, J. A.; King, D. S. *Chem. Phys.* **1984**, *85*, 31.
- (47) Johnston, H. S.; Heicklen, J. *J. Phys. Chem.* **1962**, *66*, 532.
- (48) Miller, W. H. *J. Am. Chem. Soc.* **1979**, *101*, 6810.
- (49) Kraemer, W. P.; Roos, B. O.; Bunker, P. R.; Jensen, P. *J. Mol. Spectrosc.* **1986**, *120*, 236.